Atmospheric Environment 62 (2012) 408–415

Contents lists available at SciVerse ScienceDirect

Atmospheric Environment

journal homepage: www.elsevier.com/locate/atmosenv

Coupling of highly explicit gas and aqueous chemistry mechanisms for use in 3-D

Diana L. Ginnebaugh*, Mark Z. Jacobson

Atmosphere/Energy Program, Department of Civil and Environmental Engineering, Jerry Yang & Akiko Yamazaki Environment & Energy Building, 473 Via Ortega, MC 4020, Stanford University, Stanford, CA 94305, USA

HIGHLIGHTS

- MCM 3.1 is coupled with CAPRAM 3.0i in SMVGEAR II.
- The module is compared to other model studies and mechanisms.
- Two gas-to-aqueous transfer reactions are added and one Henry's constant is modified.
- Computer timings confirm the module is practical for use in 3-D simulations.

ARTICLE INFO

Article history:
Received 9 March 2012
Received in revised form
6 July 2012
Accepted 24 August 2012

Keywords:
Chemical mechanism
Air pollution
Aqueous mechanism
MCM
CAPRAM
Gas mechanism

ABSTRACT

This study discusses the coupling of a near-explicit gas-phase chemical mechanism with an extensive aqueous-phase mechanism in an accurate chemical solver designed for use in 3-D models. The gas and aqueous mechanisms and the solver used are the Master Chemical Mechanism (MCM 3.1), the Chemical Aqueous Phase Radical Mechanism (CAPRAM 3.0i), and the SMVGEAR II ordinary differential solver, respectively. The MCM has over 13,500 reactions and 4600 species, whereas CAPRAM treats aqueous chemistry among 390 species and 829 reactions (including 51 gas-to-aqueous phase reactions). SMVGEAR II is a sparse-matrix Gear solver that reduces the computation time significantly while maintaining any specified accuracy. MCM has been used previously with SMVGEAR II in 3-D, and computer timings here indicate that coupling MCM with CAPRAM in SMVGEAR II is also practical. Gas- and aqueous-phase species are coupled through time-dependent dissolutional growth and dissociation equations. This method is validated with a smaller mechanism against results from a previous model intercomparison. When the smaller mechanism is compared with the full MCM-CAPRAM mechanism, some concentrations are still similar but others differ due to the greater detail in chemistry. We also expand the mechanism to include gas–aqueous transfer of two acids, glycolic acid and glyoxylic acid, and modify the glyoxal Henry's law constant from recent measurements. The average glyoxal partitioning in the cloud changed from 67% aqueous-phase to 87% aqueous-phase with the modifications. The addition of gas–aqueous transfer reactions increased the average gas-phase percentage of glycolic acid to 19% and of glyoxylic acid to 16%. This full gas-phase and aqueous-phase chemistry module is a potentially useful tool for studying air pollution in a cloud or a fog.

© 2012 Elsevier Ltd. All rights reserved.

1. Introduction

The purpose of this study is to combine a near-explicit gas-phase chemical mechanism with a detailed aqueous phase mechanism in an accurate chemical ordinary differential equation solver to understand better the transformation and fate of chemicals in the environment. Previously, many studies have combined moderately complex gas and aqueous mechanisms to simulate the fate of pollutants in clouds and aerosols (Pandis and Seinfeld, 1989; Liang and Jacob, 1997; Lurmann et al., 1997; Walcek et al., 1997; Liang and Jacobson, 1999; Poppe et al., 2001; Ervens et al., 2003; Sehili et al., 2005; Tilgner et al., 2006, 2007; Deguillaume et al., 2009; Fu et al., 2009; Tilgner and Herrmann, 2010). Generally, though, the organic chemistry in such mechanisms has been modest. Some studies using near-explicit gas-phase mechanisms have suggested that secondary organic aerosol (SOA) would be modeled more accurately if aqueous species were included (Jenkin, 2004; Johnson et al., 2004, 2005, 2006a, 2006b). Jenkin (2004) indicated that either simple partitioning coefficients governing

* Corresponding author. Tel./fax: +1 650 721 2730.
E-mail addresses: moongdes@stanford.edu (D.L. Ginnebaugh), Jacobson@stanford.edu (M.Z. Jacobson).

1352-2310/$ – see front matter © 2012 Elsevier Ltd. All rights reserved.
http://dx.doi.org/10.1016/j.atmosenv.2012.08.057

gas and aqueous transfer had to be increased by approximately two orders of magnitude or many additional aqueous reactions were needed to account for the correct organic aerosol formation.

In a first effort to improve the calculation of SOA resulting from aqueous processing of pollutants, this study combines a near-explicit gas-phase mechanism with a large aqueous-phase mechanism. The resulting model is found here to be practical to use in a 3-D airshed or global model over simulation periods of days to weeks. The module builds on previous work of Ginnebaugh et al. (2010), who combined the gas-phase MCM alone with SMVGEAR II. That version of the module was used in global-through-urban simulations and results were compared with ambient data in Jacobson and Ginnebaugh (2010). Here, we first describe the gas-phase mechanism, gas–aerosol transfer equations, aqueous mechanism, and solver used, and evaluate the module using a simplified set of reactions with results from a model intercomparison study (Barth et al., 2003a), hereafter referred to as B03ainit for just the initial conditions and B03a for both the initial conditions and chemical mechanism. We then add gas–aqueous transfer treatment for glycolic acid and glyoxylic acid and modify the Henry's constant for glyoxal based on new information. Finally, computer timings are provided.

2. Model description

2.1. Chemical mechanisms and solver

The gas phase chemical mechanism used for this study is the Master Chemical Mechanism (MCM), version 3.1(MCM, 2002; Jenkin et al., 2003; Saunders et al., 2003; Bloss et al., 2005). It includes over 13,500 kinetic and photolysis reactions and 4600 inorganic and organic species. It is coupled here to the Chemical Aqueous Phase Radical Mechanism (CAPRAM), version 3.0i (Barzaghi et al., 2005; Herrmann et al., 2005; Herrmann and Tilgner, 2007). CAPRAM 3.0i is extensive (Pilling, 2007) so it was ideal for this study. It includes organic species with two to six carbon atoms and treats the aqueous chemistry among 390 species and 829 reactions, including 51 gas-to-aqueous phase reactions (Herrmann et al., 2005).

Atmospheric models require a balance between the complexity of the chemistry and computational time requirements. In our case, the sparse matrix ordinary differential equation (ODE) Gear solver, SMVGEAR II (Jacobson, 1998) was selected to maintain the complexity of the chemical mechanisms while requiring minimal computer time. Most of the computing time in the integration of stiff sets of chemical ODEs is during matrix decomposition and backsubstitution. The computer time requirement depends on the size of the matrix and the number of operations that must be preformed. The size of the matrix is determined by the number of species and the number of operations depends both on the number of reactions and on the number of reactants and products in each reaction. Reordering matrices can minimize the number of operations and maximize the number of multiples by zero when solving the matrix. The multiples by zero can then be eliminated in advance, reducing computer time (Jacobson and Turco, 1994). This is referred to as a sparse-matrix technique. SMVGEAR II uses sparse-matrix and vectorization techniques to reduce computer time on both scalar and vector cores without sacrificing accuracy. Table 1 indicates that the sparse matrix technique in the code reduced decomposition and backsubstitution multiplications for the combined MCM and CAPRAM mechanisms by over 99.99%. The numbers of initial and final matrix spots filled were reduced by over 99.7% and the number of multiplications during the first loop of matrix decomposition, by far the most computationally intensive loop during all matrix operations, was reduced by over 42 billion multiplications (99.9996%) each pass through it. This dramatic reduction in operations allows for the practical use in a 3-D model of the large chemical mechanisms discussed here.

Table 1
Number of operations in SMVGEAR II during a single pass through matrix decomposition and backsubstitution when treating the MCM v. 3.1 and CAPRAM v. 3.0i chemical mechanisms together for daytime activity; Note: Decomposition 1, 2 and backsubstitution 1, 2 refer to the first and second loops of matrix decomposition and backsubstitution, respectively. Order of matrix = total number of species. Total number of reactions = 14,553.

	Initial	After sparse matrix reductions	
			% reduction
Order of matrix	5051	5051	0
No. initial matrix spots filled	25,381,444	41,260	99.84
No. final matrix spots filled	25,381,444	56,659	99.78
Decomposition 1	42,611,215,075	190,091	99.9996
Decomposition 2	12,688,203	29,210	99.77
Backsubstitution 1	12,688,203	29,210	99.77
Backsubstitution 2	12,688,203	22,411	99.82

2.2. Dissolutional growth

Gas–aqueous transfer in the model is solved with time-dependent dissolutional growth equations. Dissolutional growth is a reversible process whereby a gas transfers to the surface of a droplet and then dissolves within it and often dissociates. The phase transfer reactions cover the rate of gas transfer from the bulk gas to the surface of the droplet, transfer across the surface into the droplet, and transfer from the surface inside the droplet to the bulk water in the droplet where it dissociates and/or reacts with other species. To simplify the case, we consider only a monodisperse cloud, with equal-sized droplets and equal distributions of species. The water content, however, can vary with time – so the cloud can disappear and reappear. In this case, the transfer of the species from the gas phase to the aqueous phase is described with the liquid water fraction (L, L-water/L-air), the mass transfer coefficient (k_{mt}, 1 s^{-1}) and the Henry's constant (H, M atm^{-1}) (Jacobson, 2005).

The mass transfer coefficient, k_{mt}, governs the transfer of the species between the gas and aqueous phases and depends on the gas diffusion coefficient (D_q, cm^2 s^{-1}, where the species = q) and the mass accommodation coefficient (α). D_q and α are provided by CAPRAM 3.0i. The mass transfer coefficient is defined as

$$k_{mt} = n_i 4\pi r_i D_{q,i}^{eff}$$

where n_i is the number of particles per cm^3, r_i is the radius of the particles (cm), and $D_{q,i}^{eff}$ is the effective gas diffusion coefficient (cm^2 s^{-1}) (Jacobson, 2005). The effective gas diffusion coefficient is necessary near the surface of the droplet to take into account collision geometry, sticking probability, and ventilation. For gases other than water vapor, the effective gas diffusion coefficient can be approximated as

$$D_{q,i}^{eff} \sim D_q \omega_{q,i} F_{q,L,i}$$

where $\omega_{q,i}$ is the correction for the collision geometry and sticking probability and $F_{q,L,i}$ is the correction for ventilation (Jacobson, 2005). Ventilation is only important for large drops that are falling. $F_{q,L,i} \sim 1$ in our simplified case. The collision geometry term of the correction factor, $\omega_{q,i}$, is a function of the Knudsen number, Kn, and accounts for noncontinuum-regime growth. The sticking

probability term of the correction factor depends on the accommodation coefficient, α, and considers how likely it is that a gas will stick to the droplet after the gas has diffused to the surface. The correction factor is defined as

$$\omega_{q,i} = \left\{1 + \left[\frac{1.33 + 0.7\mathrm{Kn}_{q,i}^{-1}}{1 + \mathrm{Kn}_{q,i}^{-1}} + \frac{4(1-\alpha_{q,i})}{3\alpha_{q,i}}\right]\mathrm{Kn}_{q,i}\right\}^{-1}$$

where

$$\mathrm{Kn}_{q,i} = \frac{\lambda_q}{r_i}$$

In this equation, λ_q is the mean free path of a gas molecule (cm)

$$\lambda_q = \frac{64 D_q}{5\pi\bar{v}_q}\left(\frac{m_a}{m_a + m_q}\right)$$

which is defined by the molecular weight of air (m_a, g mol^{-1}), the molecular weight of the gas species (m_q, g mol^{-1}), and the thermal speed of the gas species ($\bar{v}_q$, cm s^{-1}) (Jacobson, 2005).

The reaction rate for the forward reaction (gas to aqueous),

$$A(\mathrm{g}) \rightarrow A(\mathrm{aq})$$

is

$$R_f = Lk_{\mathrm{mt}}P_q$$

where P_q is the pressure (atm) exerted by the gas. The rate for the reverse reaction (aqueous to gas)

$$A(\mathrm{aq}) \rightarrow A(\mathrm{g})$$

is

$$R_r = \frac{Lk_{\mathrm{mt}}[A(\mathrm{aq})]}{H_q}$$

where H_q is the Henry's constant (M atm^{-1}).

CAPRAM 3.0i provided Henry's constant at 298 K and the enthalpy of the reaction, $\Delta H/R$ (K), for each phase transfer equation. The Henry's constant at T, $H_q(T)$, is calculated in CAPRAM as

$$H_q(T) = H_q(298)\exp\left(\frac{-\Delta H}{R}\left(\frac{1}{T} - \frac{1}{298}\right)\right)$$

Since the dissociation reactions are solved explicitly, effective Henry's constants are not needed.

Dissociation reactions and other reversible reactions are solved by separating them into a forward and a reverse reaction. The equilibrium constant K (M), the forward reaction rate k_f (M^{-n} s^{-1}, where n is the number of reactants minus one), the reverse reaction rate coefficient k_r (M^{-n} s^{-1}), and the activation energy for the forward reaction, Ea/R (K), are provided by CAPRAM 3.0i for each reaction at 298 K. The equilibrium constant is the forward reaction rate coefficient divided by the reverse reaction rate coefficient,

$$K = \frac{k_f}{k_r}$$

To calculate the rate for the forward and the reverse reactions separately, k_r is assumed to be the reaction rate coefficient provided, $k_r(298)$, and the forward reaction rate coefficient is calculated using k_r,

$$k_f = Kk_r$$

$k_f(T)$ can then be calculated for varying T using the activation energy

$$k_f(T) = A\exp\left(\frac{C}{T}\right)$$

where

$$A = Kk_r\exp\left(\frac{Ea/R}{298}\right)$$

$$C = \frac{-Ea}{R}$$

A cloud or moist aerosols must be present for the aqueous reactions to take place. The module was set up to allow the cloud or moist aerosols to appear and disappear at specified times during a simulation. The liquid water fraction and either the size of the droplets (radius) or the number of droplets (# cm^{-3}) are specified to initialize the cloud. For our simulations, the liquid water fraction varied with time while the number of cloud droplets was assumed to remain constant. The cloud droplet radius was allowed to change with changes in liquid water content.

3. Model evaluation

To evaluate the model treatments of gas–aqueous transfer and basic chemistry, a relatively small gas–aqueous chemical mechanism from B03a was first substituted for the full MCM-CAPRAM mechanism in SMVGEAR II. Results from the calculations were evaluated against results from a suite of 7 gas–aqueous models previously intercompared in B03a. Two cases were examined – one with and one without a cloud – using B03a. The model with the MCM-CAPRAM mechanism was then run with B03ainit to determine whether the simplified chemistry could represent concentration changes similarly to more complete chemistry.

3.1. Model set up

The box model was set up for constant, noontime photolysis rate coefficients at 45°N, and run from 11 am to 1 pm at 1.5 km above ground level during the summer solstice. The temperature was held constant at 285 K. Two cases were considered – one with clear-sky-only (no cloud) and one with a cloud from 11:30 am to 12:30 pm. The liquid water content and pH were held constant at 0.3 g m^{-3} and 5, respectively, during cloud presence and a monodisperse cloud drop radius of 10 μm was assumed. To take into account the refraction of light within the droplets when the cloud was present, the aqueous-phase photolysis rates were increased by a factor of 1.5, as specified by B03a. The gas and aqueous phase reactions, initial concentrations, and accommodation coefficients are provided in B03a and the corresponding website (Barth et al., 2003b). The chemical mechanism included 22 gas-phase species, 33 gas-phase reactions, 25 aqueous-phase species, 25 aqueous irreversible reactions, 6 aqueous reversible reactions, and 14 gas-to-aqueous reactions.

3.2. Results and discussion

The model results for clear and cloudy-sky simulations using the chemical mechanism from B03a (B03a w/SMVGEAR II) and MCM-CAPRAM (MCM-CAPRAM w/SMVGEAR II), both with the dissolutional growth process governing the transfer of species between

the gas and aqueous phases, are shown in Figs. 1 and 2. The figure also shows the range of results from the 7 models compared in B03a for the clear and cloudy-sky simulations. The B03a simulations are in line with the shaded areas for all species.

The shapes of the results from the more extensive MCM-CAPRAM simulations are similar to those from the B03a simulations in all cases. However, the exact concentrations are often outside the shaded areas, pointing to differences between the complex and simplified mechanisms. The concentrations differed by up to 86% (NO_3) for the clear simulations and up to 145% (N_2O_5) for the cloudy simulations. For example, the MCM-CAPRAM results for methylhydroperoxide (CH_3OOH) are outside the shaded areas and differ from B03a by up to 18% for the clear simulation and 12% for the cloudy simulation. B03a and MCM both have the following gas-phase reactions for CH_3OOH:

$$CH_3OOH + OH \rightarrow CH_3O_2$$

$$CH_3OOH + OH \rightarrow HCHO + OH$$

However, the reaction rate coefficients for these reactions are 31% and 15% larger, respectively, in the B03a mechanism than in the MCM mechanism at 285 K. The actual reaction rate coefficient for this reaction is uncertain because there is large discrepancy in the measured values (IUPAC, 2007). The reaction rate coefficients in the MCM mechanism are within 5% of the measured reaction rate coefficients from Vaghjiani and Ravishankara (1989). However, both MCM and B03a reaction rate coefficients are between 14% and 53% smaller than the preferred reaction rate coefficients put forward by the International Union of Pure and Applied Chemistry (2007).

In addition, the two mechanisms have different products when CH_3OOH reacts in sunlight:

$$CH_3OOH + h\nu \rightarrow HCHO + OH + HO_2 \quad \text{(B03a)}$$

$$CH_3OOH + h\nu \rightarrow CH_3O + OH \quad \text{(MCM)}$$

The photolysis rate coefficient is 34% larger in the B03a mechanism than in the MCM mechanism. There are many additional differences in the aqueous reactions for CH_3OOH (aq) alone between B03a and the CAPRAM mechanism, including many additional aqueous reactions in the CAPRAM mechanism. Differences arise for other species as well. The combination of these differences leads to the differences in the results between the B03a case and the MCM-CAPRAM case.

4. Aqueous chemical mechanism expansion

Glyoxal is important because it is often present in the troposphere in both the gas phase and in aerosols, and it impacts secondary organic aerosol formation (SOA) (Khwaja, 1995; Kawamura et al., 1996; Limbeck and Puxbaum, 1999; Limbeck et al., 2001; Decesari et al., 2006; Ho et al., 2006; Ortiz et al., 2006; Wang et al., 2006; Carlton et al., 2007; Fu et al., 2008; Sinreich et al., 2010; Tan et al., 2010). Using CAPRAM, Tilgner and Herrmann (2010) identified glyoxal as one of the important gas phase precursors to carbonyl compounds and acids in clouds.

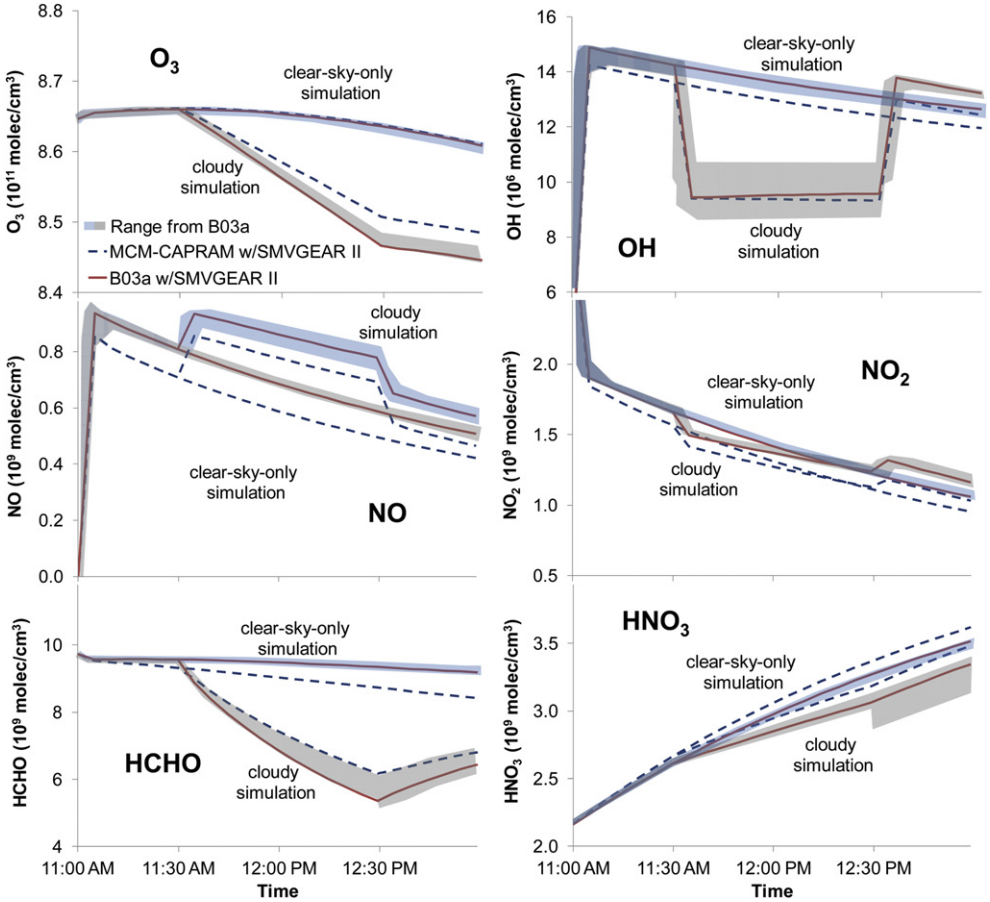

Fig. 1. Total (gas plus aqueous, including dissociation species) concentrations of selected species for clear-sky-only and cloudy-sky model simulations using the B03a mechanism (B03a w/SMVGEAR II) and the MCM and CAPRAM chemical mechanisms (MCM-CAPRAM w/SMVGEAR II) compared with the range of model results (shading) from B03a.

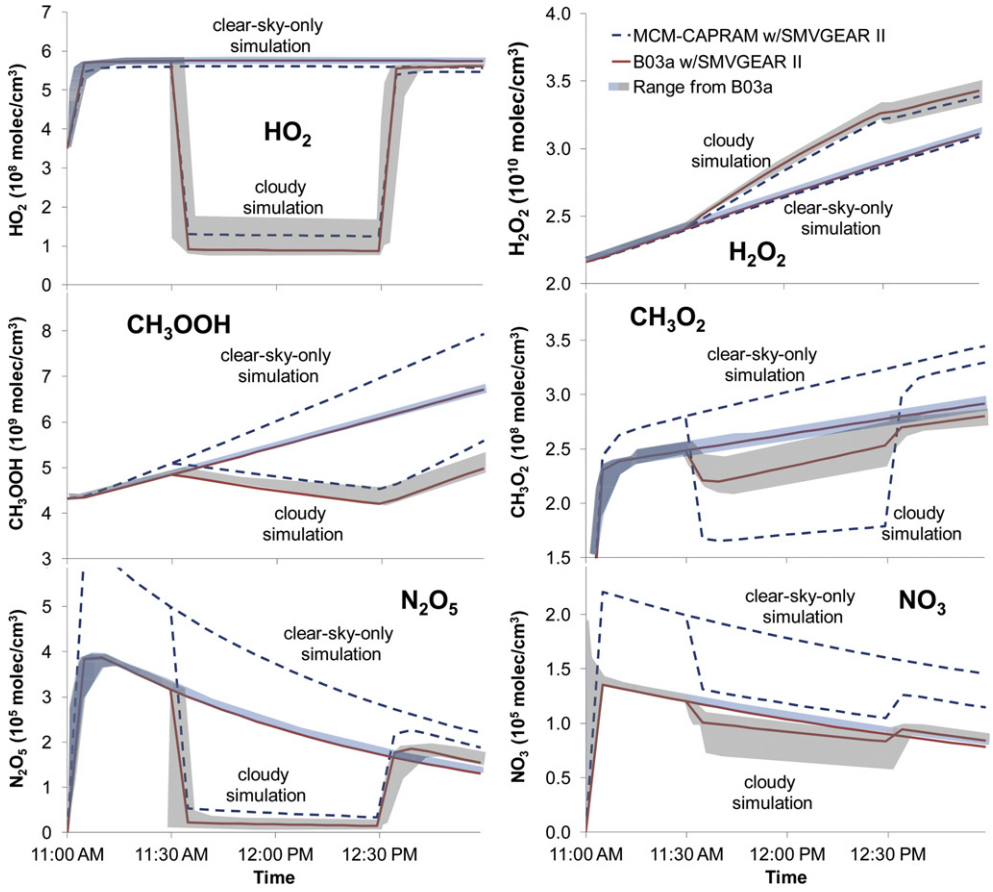

Fig. 2. Total (gas plus aqueous, including dissociation species) concentrations of additional species for clear-sky-only and cloudy-sky model simulations using the B03a mechanism (B03a w/SMVGEAR II) and the MCM and CAPRAM chemical mechanisms (MCM-CAPRAM w/SMVGEAR II) compared with the range of model results (shading) from B03a.

Ervens and Volkamer (2010) recently updated the kinetics of the glyoxal reactions using laboratory data to model better SOA from glyoxal. Here, we modify only the Henry's law constant based on new measurements from Ip et al. (2009). We also expand the CAPRAM mechanism with gas–aqueous transfer reactions for glycolic acid and glyoxylic acid based on new Henry's law constant data (Ip et al., 2009). Both of these acids already exist in the MCM for gas-phase chemistry and in the CAPRAM for aqueous phase chemistry, but no gas–aqueous transfer reactions existed for them in either mechanism (Jenkin et al., 2003; Saunders et al., 2003; Herrmann et al., 2005). Other upgrades are available for CAPRAM 3.0i, such as the free-radical chemistry summarized by Herrmann et al. (2010), but that is beyond the scope of this paper.

4.1. Aqueous chemical mechanism additions and modifications

Glyoxal (CHOCHO) was originally modeled in CAPRAM with the following parameters:

$$\mathrm{CHOCHO(g)} \leftrightarrow \mathrm{CHOCHO(aq)}$$
$$K_H(298) = 1.4\ \mathrm{M/atm}$$
$$\alpha = 0.03$$
$$D_g = 0.1\ \mathrm{cm^2/s}$$

$K_H(298)$ is the Henry's equilibrium constant at 298 K, α is the accommodation coefficient, and D_g is the gas phase diffusion coefficient. Ip et al. (2009) measured the effective Henry's equilibrium constant for glyoxal, $K'_H(298) = 4.19 \times 10^5\ \mathrm{M\ atm^{-1}}$, calculating the Henry's equilibrium constant and enthalpy of reaction as

$$K_H(298) = 1.9\ \mathrm{M/atm}$$
$$-\Delta H/R = 7481\ \mathrm{K}$$

We use the same accommodation coefficient and diffusion coefficient as provided by CAPRAM.

We added the gas-to-aqueous transfer reactions for glycolic acid ($OHCH_2CO_2H$) and glyoxylic acid ($HCOCO_2H$) based on Henry's law constant measurements from Ip et al. (2009). We also added the hydration reaction for glyoxylic acid (Sorensen et al., 1974) to link up to the existing acid dissociation reaction for hydrated glyoxylic acid in CAPRAM. We used the accommodation coefficient and diffusion coefficient from peroxy acetic acid for glycolic acid (also known as hydroxyl acetic acid) and from glyoxal for glyoxylic acid. The new data for glycolic acid and glyoxylic acid, respectively, are

$$\mathrm{OHCH_2CO_2H(g)} \leftrightarrow \mathrm{OHCH_2CO_2H(aq)}$$
$$K_H(298) = 2.37 \times 10^4\ \mathrm{M/atm}$$
$$-\Delta H/R = 4029\ \mathrm{K}$$
$$\alpha = 0.019$$
$$D_g = 0.102\ \mathrm{cm^2/s}$$

$$\mathrm{HCOCO_2H(g)} \leftrightarrow \mathrm{HCOCO_2H(aq)}$$
$$K_H(298) = 1.09 \times 10^4\ \mathrm{M/atm}$$
$$-\Delta H/R = 4811\ \mathrm{K}$$
$$\alpha = 0.03$$
$$D_g = 0.1\ \mathrm{cm^2/s}$$

$$\mathrm{HCOCO_2H(aq) + H_2O(aq)} \leftrightarrow \mathrm{CHOH_2COOH(aq)}$$
$$K_H(298) = 3.0 \times 10^2\ \mathrm{M}$$

4.2. Model set up

To investigate how the changes in Henry's constants impacted the results, we combined the cloud simulation described in B03ainit with the initial conditions, emissions, and depositions described in the rural case in Herrmann et al. (2000), hereafter referred to as H00. B03ainit has 13 initialized species while H00 has 55 initialized species including glyoxal. The conditions in H00 made the simulation complex enough to create glyoxal, glycolic, and glyoxylic acids.

4.3. Results and discussion

The modifications to the CAPRAM mechanism did not impact most species. They resulted in small changes to total (gas plus aqueous) formic acid (HCOOH) and formaldehyde (HCHO) concentrations (not shown). The time series for the total (gas plus aqueous) concentrations for clear- and cloudy-sky simulations for the modifications to glyoxal, glycolic acid, and glyoxylic acid are shown in Fig. 3. The glyoxal Henry's reaction modification had the greatest impact, increasing total glyoxylic acid concentrations by up to 29%. The other modifications had little to no impact on total gas plus aqueous glyoxal, glycolic acid, or glyoxylic acid concentrations.

The modifications, however, did change the gas–aqueous partitioning of each species. Fig. 4 shows the partitioning with the original CAPRAM mechanism and the individual modified mechanisms. More glyoxal partitioned to the aqueous phase (87%) when a cloud was present with the new Henry's constant compared to 67% with the original Henry's constant. The addition of the gas–aqueous transfer reactions for glycolic acid and glyoxylic acid allowed some of the acid produced in the cloud to partition to the gas phase. The glycolic acid originally averaged 3% gas phase (all of which was produced in the gas phase from MCM) and 97% aqueous phase from CAPRAM (all of which originated in the aqueous phase). With the addition of gas–aqueous transfer, the new partitioning was 19% gas and 81% aqueous. Similarly, the glyoxylic acid average concentrations changed from 1% gas and 99% aqueous with the original CAPRAM to 16% gas and 84% aqueous. These additions could have important implications when utilizing the MCM-CAPRAM mechanism, especially if the formation of secondary organic aerosols (SOA) is being investigated, since glyoxal is an important but often underrepresented precursor to SOA (Ervens and Volkamer, 2010).

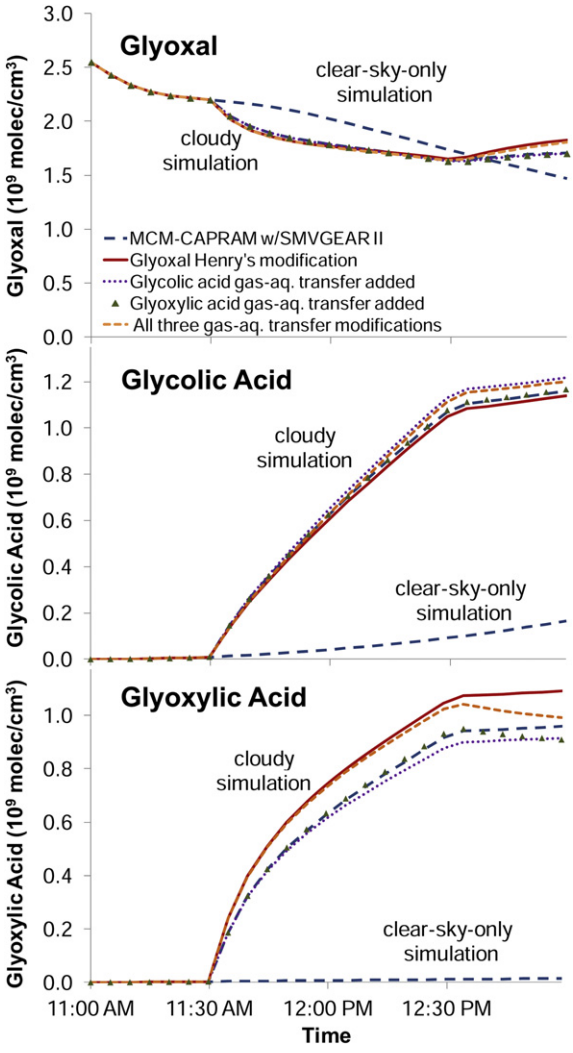

Fig. 3. Glyoxal, glycolic acid, and glyoxylic acid total (gas plus aqueous) concentrations from clear-sky-only and cloudy-sky simulations with the modification to glyoxal's Henry's constant and the addition of gas–aqueous transfer reactions for glycolic acid and glyoxylic acid.

5. Computer timings

Tests were run to estimate the computer timing of the module for photochemistry only. Ginnebaugh et al. (2010) provide previous computer timings of the MCM alone in a box model, reporting that it takes 58 s of computer run time for 24 h of model time after initialization on a single processor. Jacobson and Ginnebaugh (2010) provided timings in a realistic global-through-urban 3-D model of air pollution chemistry with the MCM, concluding that the computer time was only 3.7 times that required to solve a smaller mechanism despite factors of 31 difference in the number of species and 46 difference in the number of reactions. Here, the model was first run using the initializations from B03ainit. Three different cloud scenarios were modeled – 24 h cloud/0 h clear sky, 10 h/14 h, and 1 h/23 h. Table 2 indicates that the lifetime of the cloud had almost no impact on the computer timings. For a 24 h cloud, the MCM plus CAPRAM mechanisms required 31 s to run 24 h of model time for a box model on a single processor – a dual core xenon 5160 3.0 GHz processor with 1333 MHz cache – after initializations. This compares with 24 s for the same simulation with the MCM alone.

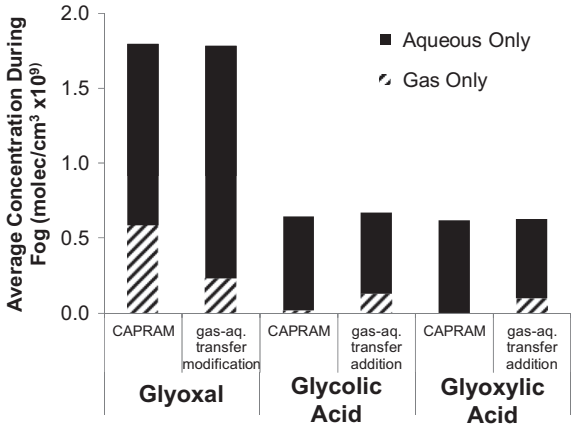

Fig. 4. Average gas phase and aqueous phase concentration of glyoxal, glycolic acid, and glyoxylic acid during the presence of the cloud in the cloudy-sky simulation with the modification to glyoxal's Henry's constant and the addition of gas–aqueous transfer reactions for glycolic acid and glyoxylic acid.

Table 2
Computer times (s, min, or days) per day of simulation on a dual-core Xeon 5160 3.0 GHz processor (1333 MHz/4 MB cache) using a simple initialization case (B03ainit) and a more complex initialization case (H00) for MCM-only and MCM-CAPRAM with SMVGEAR II with varying cloud scenarios (24 h cloud/0 h clear sky, 10 h/14 h, 1 h/23 h, and no cloud for 24 h).

	MCM w/SMVGEAR II		MCM-CAPRAM w/SMVGEAR II			
	B03ainit case	H00 case	B03ainit case			H00 case
	No cloud	No cloud	24 h cloud	10 h cloud	1 h cloud	10 h cloud
No. of reactions	13,580		14,553			
No. of species	4662		5051			
One cell (s day^{-1}) single processor	24.2	34.6	30.5	31.9	31.1	44.7
450 cells (min day^{-1}) single processor	30.1	44.9	34.8	38.5	38.4	59.4
50,000 cells (day day^{-1}) single processor	2.3	3.5	2.7	3.0	3.0	2.5
50,000 cells (min day^{-1}) parallel processor	30.1	44.9	34.8	38.5	38.4	59.4

Although the duration of the cloud does not impact the computer timing much, the complexity of the chemistry has an impact. The H00 case was used to provide more detailed initializations for the no-cloud and 10 h cloud simulations. This increased computer timings to 35 s for the no-cloud simulation and 45 s for the 10 h cloud simulation as shown in Table 2. For a 24-h simulation in 3-D with photochemistry alone, MCM-CAPRAM required 35 min over 450 grid cells without interruption for the B03ainit scenario. For comparison, MCM alone required 30 min for the same number of cells. This indicates a factor of 6.6 speedup per cell going from 1 cell to 450 cells. Since there is a speedup per cell as the number of cells increase, a simple theoretical extrapolation of these results to a 3-D global atmospheric model with 50,000 cells ($50 \times 50 \times 20$ layers) can be done. This gives 2.7 days and 2.3 days for 24 h of model time for MCM-CAPRAM and for MCM alone on a single processor. However, if each 450 cell block is put on a separate processor, the overall computer time for 50,000 grid cells is only 35 min and 30 min, respectively, since the calculations are performed in parallel. These calculations provide order-of-magnitude approximations for the computer timings. The exact timings will differ depending on the complexity of the chemistry and the type of processor.

Another way to investigate the computer timings for 3-D is to extrapolate on the actual 3-D global-through-urban simulations done with the MCM alone (Jacobson and Ginnebaugh, 2010). We found here that the MCM-CAPRAM increased computer timings over the MCM alone by a factor of approximately 1.3 for both the box and the 450 cell simulations for photochemistry only. If we assume the same factor increase for the 3-D simulations for all processes (although the photochemistry only takes about 15% of the overall computer time in this 3-D model, the additional species will take part in other processes), overall computer time required would be ~4.8 times that for a condensed mechanism, despite increases in the number of species and reactions by factors of 33 and 49, respectively. More details about the 3-D global-through-urban model and the condensed mechanism can be found in Jacobson and Ginnebaugh (2010).

6. Conclusions

This study coupled the near-explicit gas phase Master Chemical Mechanism v. 3.1, with the extensive aqueous phase Chemical Aqueous Phase Radical Mechanism v. 3.0i in the SMVGEAR II sparse matrix ordinary differential equation solver. The computer timings indicate that this solver allows these extensive chemical mechanisms to be solved in 3-D atmospheric simulations, taking only 31 s in a box model on a single processor, 35 min in a 50,000 grid cell model on parallel processors, or up to 2.7 days in a 50,000 grid cell model in serial on scalar processors for 24 h of model time (photochemistry only).

Dissolutional growth governs the gas–aqueous phase transfer and was evaluated through comparisons with 7 model results from Barth et al. (2003a). The comparison was accurate for the same mechanism. When the more extensive MCM-CAPRAM mechanism was then compared with the simplified chemistry, the concentrations of some species differed significantly due to differences in the chemical reactions. CAPRAM 3.0i was modified by updating the Henry's constant for glyoxal and adding the gas-to-aqueous transfer reactions for glycolic acid and glyoxylic acid. Glyoxal is important as a contributor to SOA and to carbonyl acids. The modification in glyoxal's Henry's constant did not impact total gas plus aqueous glyoxal much, but it did move almost all of the glyoxal to the aqueous phase in the cloud. The additional gas–aqueous reactions for glycolic acid and glyoxylic acid allowed some of the acid created in the aqueous phase to partition to the gas phase while the cloud was present. These additions to CAPRAM could be important for improving prediction of secondary organic aerosol formation. This model allows more extensive chemistry when modeling air pollution in a cloud or a fog and could improve air pollution simulations.

This model can be obtained for research purposes by e-mailing the author at moongdes@stanford.edu.

Acknowledgment

The authors would like to thank Hartmut Herrmann and Andreas Tilgner for providing information and assistance related to CAPRAM and Mary Barth for providing intercomparison information. This work was supported by the U.S. Environmental Protection Agency grant RD-83337101-O and the National Science Foundation.

References

Barth, M.C., Sillman, S., Hudman, R., Jacobson, M.Z., Kim, C.H., Monod, A., Liang, J., 2003a. Summary of the cloud chemistry modeling intercomparison: photochemical box model simulation. J. Geophys. Res. 108 (D7). http://dx.doi.org/10.1029/2002jd002673.

Barth, M.C., Sillman, S., Hudman, R., Jacobson, M.Z., Kim, C.H., Monod, A., Liang, J., 2003b. Summary of the Cloud Chemistry Modeling Intercomparison: Photochemical Box Model Simulation, Part 1. From: http://acd.ucar.edu/~barthm/Description/Cloud_Chemistry.html.

Barzaghi, P., Tilgner, A., Majdik, Z., Gligorovski, S., Poulain, L., Monod, A., Herrmann, H., 2005. CAPRAM 3.0: a mechanism with a more detailed description of tropospheric aqueous phase organic chemistry. Geophys. Res. Abs. 7 (04374).

Bloss, C., et al., 2005. Development of a detailed chemical mechanism (MCMv3.1) for the atmospheric oxidation of aromatic hydrocarbons. Atmos. Chem. Phys. 5 (3), 641–664.

Carlton, A.G., Turpin, B.J., Altieri, K.E., Seitzinger, S., Reff, A., Lim, H.-J., Ervens, B., 2007. Atmospheric oxalic acid and SOA production from glyoxal: results of aqueous photooxidation experiments. Atmos. Environ. 41 (35), 7588–7602.

Decesari, S., et al., 2006. Characterization of the organic composition of aerosols from Rondônia, Brazil, during the LBA-SMOCC 2002 experiment and its representation through model compounds. Atmos. Chem. Phys. 6 (2), 375–402.

Deguillaume, L., Tilgner, A., Schrodner, R., Wolke, R., Chaumerliac, N., Herrmann, H., 2009. Towards an operational aqueous phase chemistry mechanism for regional chemistry-transport models: CAPRAM-RED and its application to the COSMO-MUSCAT model. J. Atmos. Chem. 64 (1), 1–35. http://dx.doi.org/10.1007/s10874-010-9168-8.

Ervens, B., Volkamer, R., 2010. Glyoxal processing by aerosol multiphase chemistry: towards a kinetic modeling framework of secondary organic aerosol formation in aqueous particles. Atmos. Chem. Phys. 10, 8219–8244. http://dx.doi.org/10.5194/acp-10-8219-2010.

Ervens, B., et al., 2003. CAPRAM 2.4 (MODAC mechanism): an extended and condensed tropospheric aqueous phase mechanism and its application. J. Geophys. Res. 108 (D14). http://dx.doi.org/10.1029/2002JD002202

Fu, T.-M., Jacob, D.J., Wittrock, F., Burrows, J.P., Vrekoussis, M., Henze, D.K., 2008. Global budgets of atmospheric glyoxal and methylglyoxal, and implications for formation of secondary organic aerosols. J. Geophys. Res. 113 (D15), D15303. http://dx.doi.org/10.1029/2007jd009505.

Fu, T.-M., Jacob, D.J., Heald, C.L., 2009. Aqueous-phase reactive uptake of dicarbonyls as a source of organic aerosol over eastern North America. Atmos. Environ. 43 (10), 1814–1822. http://dx.doi.org/10.1016/j.atmosenv.2008.12.029.

Ginnebaugh, D.L., Liang, J., Jacobson, M.Z., 2010. Examining the temperature dependence of ethanol (E85) versus gasoline emissions on air pollution with a largely-explicit chemical mechanism. Atmos. Environ. 44, 1192–1199. http://dx.doi.org/10.1016/j.atmosenv.2009.12.024.

Herrmann, H., Ervens, B., Jacobi, H.-W., Wolke, R., Nowacki, P., Zellner, R., 2000. CAPRAM 2.3: a chemical aqueous phase radical mechanism for tropospheric chemistry. J. Atmos. Chem. 36 (3), 231–284.

Herrmann, H., Tilgner, A., Barzaghi, P., Majdik, Z., Gligorovski, S., Poulain, L., Monod, A., 2005. Towards a more detailed description of tropospheric aqueous phase organic chemistry: CAPRAM 3.0. Atmos. Environ. 39 (23–24), 4351–4363.

Herrmann, H., Tilgner, A., 2007. CAPRAM (=Chemical Aqueous Phase RAdical Mechanism). From: http://projects.tropos.de/capram/index.html.

Herrmann, H., Hoffmann, D., Schaefer, T., Bräuer, P., Tilgner, A., 2010. Tropospheric aqueous-phase free-radical chemistry: radical sources, spectra, reaction kinetics and prediction tools. ChemPhysChem 11 (18), 3796–3822. http://dx.doi.org/10.1002/cphc.201000533.

Ho, K.F., Lee, S.C., Cao, J.J., Kawamura, K., Watanabe, T., Cheng, Y., Chow, J.C., 2006. Dicarboxylic acids, ketocarboxylic acids and dicarbonyls in the urban roadside area of Hong Kong. Atmos. Environ. 40 (17), 3030–3040. http://dx.doi.org/10.1016/j.atmosenv.2005.11.069.

Ip, H.S.S., Huang, X.H.H., Yu, J.Z., 2009. Effective Henry's law constants of glyoxal, glyoxylic acid, and glycolic acid. Geophys. Res. Lett. 36 (L01802). http://dx.doi.org/10.1029/2008GL036212.

IUPAC, 2007. International Union of Pure and Applied Chemistry. From: http://www.iupac-kinetic.ch.cam.ac.uk/.

Jacobson, M.Z., Ginnebaugh, D.L., 2010. The global-through-urban nested 3-D simulation of air pollution with a 13,600-reaction photochemical mechanism. J. Geophys. Res. 115 (D14304). http://dx.doi.org/10.1029/2009JDO13289.

Jacobson, M.Z., Turco, R.P., 1994. SMVGEAR: a sparse-matrix, vectorized gear code for atmospheric models. Atmos. Environ. 28 (2), 273–284.

Jacobson, M.Z., 1998. Improvement of SMVGEAR II on vector and scalar machines through absolute error tolerance control. Atmos. Environ. 32 (4), 791–796.

Jacobson, M.Z., 2005. Fundamentals of Atmospheric Modeling, second ed. Cambridge University Press, New York.

Jenkin, M.E., Saunders, S.M., Wagner, V., Pilling, M.J., 2003. Protocol for the development of the Master Chemical Mechanism, MCM v3 (part B): tropospheric degradation of aromatic volatile organic compounds. Atmos. Chem. Phys. Discuss. 2, 1905–1938.

Jenkin, M.E., 2004. Modelling the formation and composition of secondary organic aerosol from a- and b-pinene ozonolysis using MCM v3. Atmos. Chem. Phys. Discuss. 4, 2905–2948.

Johnson, D., Jenkin, M.E., Wirtz, K., Martin-Reviejo, M., 2004. Simulating the formation of secondary organic aerosol from the photooxidation of toluene. Environ. Chem. 1 (3), 150–165.

Johnson, D., Jenkin, M.E., Wirtz, K., Martin-Reviejo, M., 2005. Simulating the formation of secondary organic aerosol from the photooxidation of aromatic hydrocarbons. Environ. Chem. 2 (1), 35–48.

Johnson, D., Utembe, S.R., Jenkin, M.E., 2006a. Simulating the detailed chemical composition of secondary organic aerosol formed on a regional scale during the TORCH 2003 campaign in the southern UK. Atmos. Chem. Phys. 6 (2), 419–431.

Johnson, D., Utembe, S.R., Jenkin, M.E., Derwent, R.G., Hayman, G.D., Alfarra, M.R., Coe, H., McFiggans, G., 2006b. Simulating regional scale secondary organic aerosol formation during the TORCH 2003 campaign in the southern UK. Atmos. Chem. Phys. 6 (2), 403–418.

Kawamura, K., Kasukabe, H., Barrie, L.A., 1996. Source and reaction pathways of dicarboxylic acids, ketoacids and dicarbonyls in arctic aerosols: one year of observations. Atmos. Environ. 30 (10–11), 1709–1722. http://dx.doi.org/10.1016/1352-2310(95)00395-9.

Khwaja, H.A., 1995. Atmospheric concentrations of carboxylic acids and related compounds at a semiurban site. Atmos. Environ. 29 (1), 127–139. http://dx.doi.org/10.1016/1352-2310(94)00211-3.

Liang, J., Jacob, D.J., 1997. Effect of aqueous phase cloud chemistry on tropospheric ozone. J. Geophys. Res. 102 (D5), 5993–6001. http://dx.doi.org/10.1029/96jd02957.

Liang, J., Jacobson, M.Z., 1999. A study of sulfur dioxide oxidation pathways over a range of liquid water contents, pH values, and temperatures. J. Geophys. Res. 104 (D11), 12749–13769.

Limbeck, A., Puxbaum, H., 1999. Organic acids in continental background aerosols. Atmos. Environ. 33 (12), 1847–1852. http://dx.doi.org/10.1016/s1352-2310(98)00347-1.

Limbeck, A., Puxbaum, H., Otter, L., Scholes, M.C., 2001. Semivolatile behavior of dicarboxylic acids and other polar organic species at a rural background site (Nylsvley, RSA). Atmos. Environ. 35 (10), 1853–1862. http://dx.doi.org/10.1016/s1352-2310(00)00497-0.

Lurmann, F.W., Wexler, A.S., Pandis, S.N., Musarra, S., Kumar, N., Seinfeld, J.H., 1997. Modelling urban and regional aerosols—II. Application to California's South Coast Air Basin. Atmos. Environ. 31 (17), 2695–2715. http://dx.doi.org/10.1016/s1352-2310(97)00100-3.

MCM. University of LEEDS, 2002. Master Chemical Mechanism V. 3.1. From: http://mcm.leeds.ac.uk/MCMv3.1/.

Ortiz, R., Hagino, H., Sekiguchi, K., Wang, Q., Sakamoto, K., 2006. Ambient air measurements of six bifunctional carbonyls in a suburban area. Atmos. Res. 82 (3–4), 709–718. http://dx.doi.org/10.1016/j.atmosres.2006.02.025.

Pandis, S.N., Seinfeld, J.H., 1989. Sensitivity analysis of a chemical mechanism for aqueous-phase atmospheric chemistry. J. Geophys. Res. 94 (D1), 1105–1126. http://dx.doi.org/10.1029/JD094iD01p01105.

Pilling, M.J., 2007. Representation of chemical detail in atmospheric models. In: Regional Climate Variability and its Impacts in the Mediterranean Area, Proceedings of the NATO Advanced Research Workshop. Marrakech, Morocco, vol. 79, pp. 207–218.

Poppe, D., et al., 2001. Scenarios for modeling multiphase tropospheric chemistry. J. Atmos. Chem. 40 (1), 77–86. http://dx.doi.org/10.1023/a:1010678609413.

Saunders, S.M., Jenkin, M.E., Derwent, R.G., Pilling, M.J., 2003. Protocol for the development of the Master Chemical Mechanism, MCM v3 (part A): tropospheric degradation of non-aromatic volatile organic compounds. Atmos. Chem. Phys. 3, 161–180.

Sehili, A.M., Wolke, R., Knoth, O., Simmel, M., Tilgner, A., Herrmann, H., 2005. Comparison of different model approaches for the simulation of multiphase processes. Atmos. Environ. 39 (23–24), 4403–4417.

Sinreich, R., Coburn, S., Dix, B., Volkamer, R., 2010. Ship-based detection of glyoxal over the remote tropical Pacific Ocean. Atmos. Chem. Phys. 10, 11359–11371. http://dx.doi.org/10.5194/acp-10-11359-2010.

Sorensen, P.E., Bruhn, K., Lindelov, F., 1974. Kinetics and equilibria for the reversible hydration of the aldehyde group in glyoxylic acid. Acta Chem. Scand. A 28, 162–168.

Tan, Y., Carlton, A.G., Seitzinger, S.P., Turpin, B.J., 2010. SOA from methylglyoxal in clouds and wet aerosols: measurement and prediction of key products. Atmos. Environ. 44 (39), 5218–5226.

Tilgner, A., Herrmann, H., 2010. Radical-driven carbonyl-to-acid conversion and acid degradation in tropospheric aqueous systems studied by CAPRAM. Atmos. Environ. 44 (40), 5415–5422.

Tilgner, A., Wolke, R., Herrmann, H., 2006. SPACCIM model studies of the multiphase aerosol processing in warm tropospheric clouds. Geophys. Res. Abs. 8 (04107).

Tilgner, A., Wolke, R., Herrmann, H., 2007. SPACCIM model studies on the multiphase processing of tropospheric aerosols. Geophys. Res. Abs. 9 (03991).

Vaghjiani, G.L., Ravishankara, A.R., 1989. Kinetics and mechanism of hydroxyl radical reaction with methyl hydroperoxide. J. Phys. Chem. 93 (5), 1948–1959. http://dx.doi.org/10.1021/j100342a050.

Walcek, C.J., Yuan, H.-H., Stockwell, W.R., 1997. The influence of aqueous-phase chemical reactions on ozone formation in polluted and nonpolluted clouds. Atmos. Environ. 31 (8), 1221–1237. http://dx.doi.org/10.1016/s1352-2310(96)00257-9.

Wang, H., Kawamura, K., Yamazaki, K., 2006. Water-soluble dicarboxylic acids, ketoacids and dicarbonyls in the atmospheric aerosols over the southern ocean and western Pacific Ocean. J. Atmos. Chem. 53 (1), 43–61. http://dx.doi.org/10.1007/s10874-006-1479-4.